

Canonical analytical solutions of wave-induced thermoelastic attenuation

José M. Carcione,^{1,2} Davide Gei,¹ Juan E. Santos,^{2,3,4} Li-Yun Fu⁵ and Jing Ba²

¹*Istituto Nazionale di Oceanografia e di Geofisica Sperimentale (OGS), Borgo Grotta Gigante 42c, Sgonico 34010, Trieste, Italy*

²*School of Earth Sciences and Engineering, Hohai University, Nanjing 210023, China. E-mail: jba@hhu.edu.cn*

³*Facultad de Ingeniería, Instituto del Gas y del Petróleo, Universidad de Buenos Aires, Av. Las Heras 2214, Piso 3, Buenos Aires C1127AAR, Argentina*

⁴*Department of Mathematics, Purdue University, 150 N. University Street, West Lafayette, IN 47907-2067, USA*

⁵*School of Geosciences, China University of Petroleum (East China), Qingdao 266580, China*

Accepted 2020 January 13. Received 2020 January 5; in original form 2019 September 17

SUMMARY

Thermoelastic attenuation is similar to wave-induced fluid-flow attenuation (mesoscopic loss) due to conversion of the fast P wave to the slow (Biot) P mode. In the thermoelastic case, the P - and S -wave energies are lost because of thermal diffusion. The thermal mode is diffusive at low frequencies and wave-like at high frequencies, in the same manner as the Biot slow mode. Therefore, at low frequencies, that is, neglecting the inertial terms, a mathematical analogy can be established between the diffusion equations in poroelasticity and thermoelasticity. We study thermoelastic dissipation for spherical and cylindrical cavities (or pores) in 2-D and 3-D, respectively, and a finely layered system, where, in the latter case, only the Grüneisen ratio is allowed to vary. The results show typical quality-factor relaxation curves similar to Zener peaks. There is no dissipation when the radius of the pores tends to zero and the layers have the same properties. Although idealized, these canonical solutions are useful to study the physics of thermoelasticity and test numerical algorithm codes that simulate thermoelastic dissipation.

Key words: Elasticity and anelasticity; Body waves; Seismic attenuation; Wave propagation.

1 INTRODUCTION

The theory of thermoelasticity is based on the heat equation coupled with the theory of dynamic elasticity, specifically, it describes the relation between the fields of stress-deformation and temperature. The theory is relevant for geophysical studies such as seismic attenuation (Zener 1938; Treitel 1959; Savage 1966; Armstrong 1984). Basically, a source of elastic waves induces a temperature field and heat flow equalizes the temperature difference with the surroundings giving rise to the energy dissipation. Similarly, a heat source generates viscoelastic waves and anelastic deformations.

Biot (1956) used the differential equations based on the Fourier law of heat conduction, but this formulation has unphysical solutions such as discontinuities and infinite velocities as a function of frequency, since it is based on a parabolic-type differential equation. This behaviour is typical of pure diffusion equations. A more general (physical) system of equations is based on a hyperbolic heat equation. Carcione *et al.* (2018b) used the equations of Lord & Shulman (1967) to obtain finite phase velocities at all frequencies and compute synthetic seismograms. Carcione *et al.* (2019) generalized these equations to the poroelastic case by combining Biot's equations (e.g. Carcione 2014) with those of Lord & Shulman (1967). The thermoelastic theory predicts two P waves and an S wave, the latter not affected by the thermal effects in the homogeneous case.

The P waves are an elastic wave (E wave) and a thermal wave (T wave) having similar characteristics to the fast and slow P waves of poroelasticity (e.g. Carcione 2014). Indeed, Carcione *et al.* (2019) show that the Biot slow wave and the thermal wave co-exist and have the same behaviour, that is, diffusive at low frequencies and wave-like at high frequencies.

In geophysical applications, both the thermal wave and the Biot slow P wave are diffusive. The diffusive character of the Biot wave is the cause of attenuation of the fast P wave by means of the mechanism called mesoscopic attenuation or wave-induced fluid-flow attenuation (e.g. Müller *et al.* 2010). Energy transfer between wave modes, with P -wave to slow P (Biot)-wave conversion being the main physical mechanism. The mesoscopic-scale length is intended to be larger than the grain sizes but much smaller than the wavelength of the pulse. In the thermoelastic case, the heterogeneities and/or cracks or cavities are much smaller than the signal wavelength. Zener (1938) explained the physics of thermoelastic attenuation in homogeneous media: 'Stress inhomogeneities in a vibrating body give rise to fluctuations in temperature, and hence to local heat currents. These heat currents increase the entropy of the vibrating solid, and hence are a source of internal friction'. Basically, the temperature variation caused by the passage of the P wave provides the gradient from which the thermal dissipation and attenuation occur. Zener (1946) anticipated the concept of attenuation

due to diffusion, where he mentions thermal, atomic and magnetic diffusion as the causes. The Biot slow mode represents loss due to fluid-pressure diffusion.

Moreover, Armstrong (1984) found that the distribution and correlation of heterogeneities play an important role in the determination of the frequency dependence of thermal dissipation, and here the wave conversion is an additional loss mechanism. At low frequencies, the thermal mode is diffusive and is responsible for the attenuation and velocity dispersion of the P and S waves. Since the inertial terms are neglected, as in the mesoscopic-loss case [see eq. (6) in Carcione *et al.* (2011) and Chapter 7 in Santos & Gauzellino (2017)], the equation to be solved is of purely diffusive type.

We first establish the analogy between the diffusion equations in poroelasticity and thermoelasticity, and then study the solutions proposed by Savage (1966) for empty round pores, by Armstrong (1984) for a periodic system of thin slabs with the condition that no heat escape the system, and boundary conditions that impose continuity of temperature and thermal current across the slab boundaries. Savage (1966)'s theory underestimates attenuation in rocks, possibly due to the fact that cracks do not interact. He reports an error in Zener (1938)'s eq. (18), for computing the dilation due to a shear strain in the presence of spherical cavities. In this case, P and S waves suffer attenuation and dispersion due to shear loss, while there are no losses due to dilatational deformations. On the other hand, Armstrong (1984) provides the solution for the P -wave quality factor across a set of periodic layers.

In all the cases, we use a method proposed by O'Donnell *et al.* (1981), based on the Kramers–Kronig relations (e.g. Carcione *et al.* 2018a) to obtain the phase velocities and complex moduli.

2 DIFFUSION EQUATION OF THERMOELASTICITY AND ANALYTICAL SOLUTIONS

Let us define by ϵ_{ij} , $i, j = 1, 2, 3$ the components of the strain field, by σ_{ij} the components of the stress tensor and by T the increment of temperature above a reference absolute temperature T_0 for the state of zero stress and strain. In a linear isotropic medium, the stress–strain relations of thermoelasticity are given by [Biot (1956), eq. (2.2)]

$$\sigma_{ij} = 2\mu\epsilon_{ij} + (\lambda\epsilon - \beta T)\delta_{ij}, \quad (1)$$

where ϵ is the trace of the strain tensor, λ and μ are the Lamé constants,

$$\beta = (3\lambda + 2\mu)\alpha = 3\alpha K, \quad (2)$$

K is the bulk modulus, α is the coefficient of linear thermal expansion (the volumetric one is 3α ; e.g. Carcione *et al.* 2018b) and δ_{ij} is Kronecker's delta. If we neglect inertial terms, the stress equilibrium equation is

$$\partial_i \sigma_{ij} = 0 \quad (3)$$

[Biot (1956), eq. (10.1)].

The law of heat conduction is

$$\gamma \Delta T = c\dot{T} + \beta T_0 \dot{\epsilon} \quad (4)$$

[Landau & Lifshitz (1970), eq. (32.2); Mainardi (2010), eq. (3.43)], where γ is the coefficient of heat conduction (or thermal conductivity), c is the specific heat per unit volume, Δ is the Laplacian and a dot above a variable denotes time derivative. (In many publications $c = \rho C$ and $3\alpha = \alpha_v$, being C and α_v the specific heat and volumetric

thermal expansion, respectively, and ρ is the mass density). Eq. (4) assumes that the change in temperature is small and proportional to the trace of the strain tensor [Landau & Lifshitz (1970), eq. (6.3)], that is, variations in temperature-induced volume changes, provided that the medium is homogeneous.

Since there are several distinct definitions of the thermoelastic constants in the literature [e.g. compare eq. (4) to that of Savage (1966)], we indicate here the units of the different constants in the MKS system:

$$\begin{aligned} \lambda, \mu, K &\rightarrow \text{kg m}^{-1} \text{s}^{-2} \text{ (or Pa)}, \\ \gamma &\rightarrow \text{m kg s}^{-3} \text{K}^{-1}, \\ c &\rightarrow \text{kg m}^{-1} \text{s}^{-2} \text{K}^{-1}, \\ \beta &\rightarrow \text{kg m}^{-1} \text{s}^{-2} \text{K}^{-1}, \\ \alpha &\rightarrow \text{K}^{-1}, \\ T_0 &\rightarrow \text{K}. \end{aligned} \quad (5)$$

The analogy between poroelasticity and thermoelasticity is established in Appendix A. Both fields obey a diffusion equation at low frequencies when neglecting inertial (acceleration) terms. The analogy identifies temperature with fluid pressure and thermal diffusivity, d_t , with hydraulic diffusivity, d_h , such that

$$d_t = \left(\frac{\gamma}{c + \beta^2 T_0 / E} \right) \longleftrightarrow M \left(\frac{\kappa}{\eta} \right) \left(\frac{K_m + 4\mu_m / 3}{K_G + 4\mu_m / 3} \right) = d_h, \quad (6)$$

where the properties are defined in Appendix A. Basically, there is a correspondence between the quantities γ and $1/\eta$, that is, the heat and fluid fluxes increase with increasing thermal conductivity and decreasing fluid viscosity. Both thermal diffusivities have units of $\text{m}^2 \text{s}^{-1}$. The thermal diffusivity relates the adiabatic and isothermal P -wave moduli as $E_A = E_d/c$ (see Appendix A). Typical values are 1.3, 1.1 and $0.8 \text{ mm}^2 \text{ s}^{-1}$ for sandstone, limestone and shale, compared to 0.15, 20 and $114 \text{ mm}^2 \text{ s}^{-1}$ for water, air and copper (Robertson 1988).

Appendices B and C provide the solutions for the quality factors obtained by Savage (1966) for empty round cavities or pores and by Armstrong (1984) for a periodic finely layered medium. In poroelasticity, the mesoscopic-loss mechanism is associated with the presence of the Biot slow wave. The critical fluid-diffusion relaxation length is $L = \sqrt{d_h/\omega}$ (Carcione 2014, section 7.13). The fluid pressures will be equilibrated if L is comparable to the period of the stratification. For smaller diffusion lengths (e.g. higher frequencies), the pressures will not be equilibrated, causing attenuation and velocity dispersion. In thermoelasticity, the heat currents induced by the mechanical waves have a diffusion length $L = \sqrt{d_t/\omega}$. When this length has the size of the pores or layers, maximum attenuation is expected.

To obtain the phase velocity, we use an approximation reported by O'Donnell *et al.* (1981), based on the Kramers–Kronig relations (Carcione *et al.* 2018a). The phase velocity, c_{ph} is related to the attenuation factor, A , as

$$\frac{1}{c_0} - \frac{1}{c_{\text{ph}}(\omega)} = \frac{2}{\pi} \int_{\omega_0}^{\omega} \frac{A(\omega')}{\omega'^2} d\omega', \quad (7)$$

where c_0 is a reference velocity at ω_0 that can be assumed the low-frequency limit ($\omega_0 \approx 0$). For low-loss solids ($Q \gg 1$), we have $A \approx \omega/(2c_0 Q)$ and

$$\frac{c_0}{c_{\text{ph}}(\omega)} = 1 - \frac{1}{\pi} \int_{\omega_0}^{\omega} \frac{Q^{-1}(\omega')}{\omega'} d\omega'. \quad (8)$$

We can get the complex wave modulus, P , from the phase velocity and Q factor, where P can be the shear or the P -wave complex

modulus. Define

$$P = P_R + P_I = (p + iq)^2, \quad (9)$$

where the subindices denote real and imaginary parts. Then

$$P_R = p^2 - q^2, \quad \text{and} \quad P_I = 2pq. \quad (10)$$

Since the phase velocity satisfies $\rho c_{\text{ph}}^2 \approx \text{Re}^2(\sqrt{P}) = p^2$ (for $Q \gg 1$) and $P_R = QP_I$, we obtain $q \approx p/(2Q)$. Hence, $P_R = p^2[1 - 1/(4Q^2)]$ and $P_I = p^2/Q$, so that

$$P(\omega) = \rho c_{\text{ph}}^2 \left(1 - \frac{1}{4Q^2} + \frac{i}{Q}\right) \approx \rho c_{\text{ph}}^2(\omega) \left(1 + \frac{i}{Q(\omega)}\right). \quad (11)$$

If the complex shear and P -wave moduli obtained above are μ_c and $E_c = K_c + 4\mu_c/3$, where K_c is the complex modulus, this is given by $K_c = E_c - 4\mu_c/3$.

3 EXAMPLES

The medium considered by Savage (1966) is granite, but the values of K/\bar{K} and σ (Poisson ratio) assumed by him lead to a porosity greater than 1 according to eq. (B3), so we discard this example. Actually, the theory holds for small porosities, since the cavities do not interact (Eshelby 1957). Here, we assume an ideal medium with a high thermal expansion coefficient, to obtain a high dissipation, and the following properties:

$$\begin{aligned} \alpha &: 10^{-3} \text{ K}^{-1} \\ \gamma/c &: 5 \times 10^{-6} \text{ m}^2 \text{ s}^{-1} \\ \Gamma = \beta/c &: 1.1 \\ K/\bar{K} &: 1.18 \\ \sigma &: 0.17 \\ K &: 39 \text{ GPa} = 39 \times 10^9 \text{ kg m}^{-1} \text{ s}^{-2} \\ a &: 0.2 \text{ mm} = 0.0002 \text{ m} \\ T_0 &: 300 \text{ K}. \end{aligned} \quad (12)$$

The porosity and $\bar{\mu}/\mu$ can be obtained from eq. (B3), with

$$\phi = \frac{1}{3} \left(\frac{K}{\bar{K}} - 1 \right) \frac{2 - 4\sigma}{1 - \sigma}. \quad (13)$$

For spherical voids, we obtain $\phi = 9.5$ per cent, $\mu/\bar{\mu} = 1.19$, $\beta = 3\alpha K = 117 \times 10^6 \text{ kg m}^{-1} \text{ s}^{-2} \text{ K}$, $c = \beta/\Gamma = 106 \times 10^6 \text{ kg m}^{-1} \text{ s}^{-2} \text{ K}$, $\gamma = 532 \text{ m kg s}^{-3} \text{ K}$, $\bar{K} = 33 \text{ GPa}$, $\mu = 33 \text{ GPa}$, $\bar{\mu} = 27.6 \text{ GPa}$, $\bar{\sigma} = 0.173$, and $\bar{E} = \bar{K} + 4\bar{\mu}/3 = 70 \text{ GPa}$ [note that $\mu = 3K(1 - 2\sigma)/(2 + 2\sigma)$] (see Appendix B for the definition of the above properties).

Fig. 1 shows the relaxation peaks corresponding to spherical pores. As can be seen, increasing the sphere radius the peaks move to the lower frequencies, but the peak dissipation factor (inverse of Q) remains constant. Zero radius implies that the peak moves to infinite and the dissipation is zero at all frequencies. Since the attenuation factor is proportional to the frequency (Carcione 2014, eq. 2.123), this factor increases almost linearly with frequency. It is believed that the Zener model (see Appendix D) is a representation of the thermoelastic peak (Zener 1938). Fig. 2 compares the S -wave and Zener dissipation factors, where f_0 and the minimum quality factor, Q_0 , is the same for both peaks, but the results are dissimilar. The comparison between the 2-D (cylindrical) and 3-D (spherical) cases is shown in Fig. 3. In the 2-D case, the dissipation is much weaker, while the peak has moved slightly to lower frequencies. Fig. 4 shows the Zener fit, which in this case is narrower than the thermoelastic curve, as in the spherical case (Fig. 2). In all the cases, the P -wave dissipation is smaller than the S -wave one.

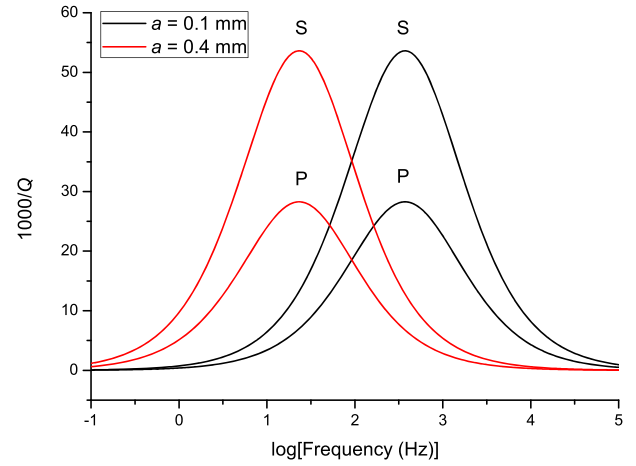


Figure 1. Dissipation factors of the P and S waves as a function of frequency for two different values of the radius of the spherical pores.

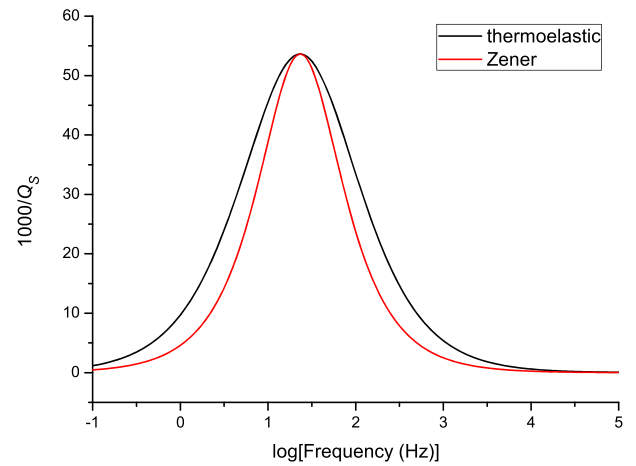


Figure 2. Comparison between the S -wave and Zener dissipation factors for spherical pores of radius $a = 0.4$ mm.

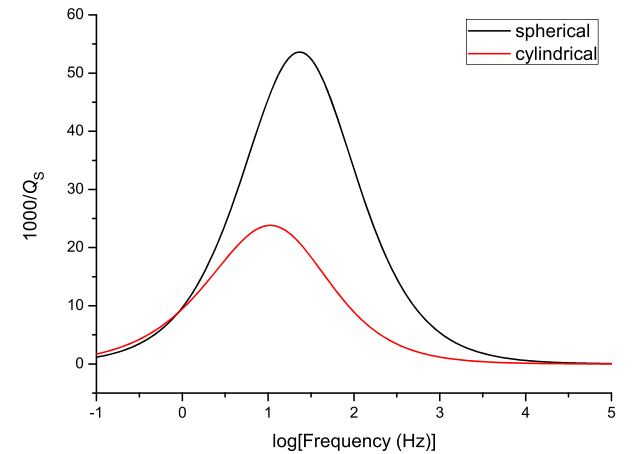


Figure 3. Dissipation factors of the S waves as a function of frequency for spherical (3-D, black) and cylindrical (2-D, red) pores. The radius is $a = 0.4$ mm.

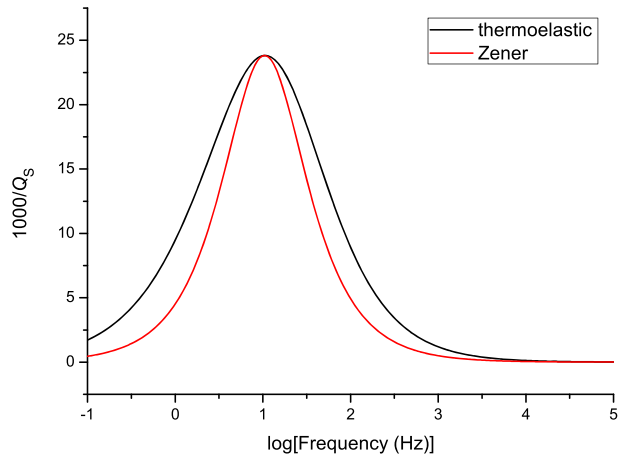


Figure 4. Comparison between the S -wave and Zener dissipation factors for cylindrical pores of radius $a = 0.4$ mm.

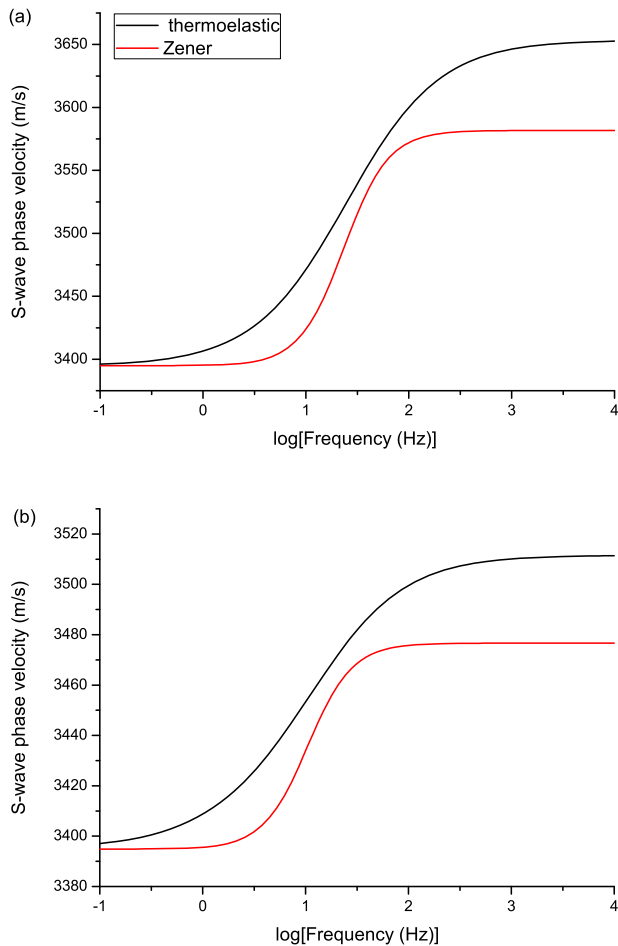


Figure 5. Comparison between the S -wave phase velocity and that of the Zener model for spherical (a) and cylindrical (b) pores, with radius $a = 0.4$ mm.

Let us compute the S -wave phase velocity of the medium. We assume a density $\rho = (1 - \phi)\rho_s \approx 2400 \text{ kg m}^{-3}$, where $\rho_s = 2650 \text{ kg m}^{-3}$. Fig. 5 shows the S -wave phase velocity as a function of frequency, compared to that of the Zener model for the 3-D (a) and 2-D (b) cases. The dispersion is stronger for the thermoelastic peaks. This is related to the width of the peaks, with the Zener one

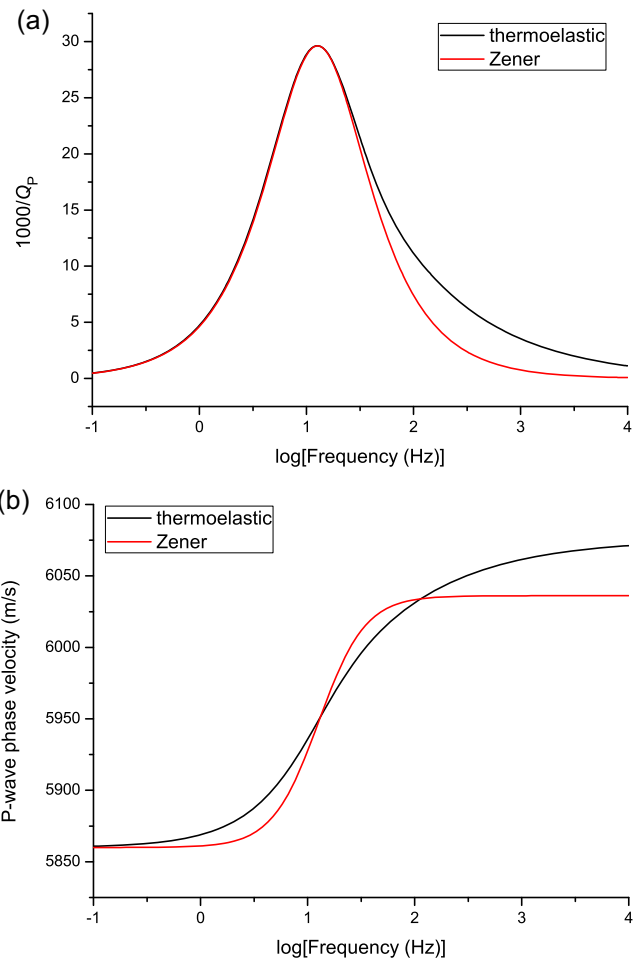


Figure 6. Dissipation factor (a) and phase velocity (b) of the P waves as a function of frequency for a periodic sequence of slabs (fine layering). The thickness is $h = 0.8$ mm (period = 0.16 mm). The Zener fit is shown.

as a reference. A narrower peak implies less velocity dispersion. An estimation of the phase-velocity dispersion based on the Zener model is approximately $\Delta c_{\text{ph}} = c_0/Q_0$ (Carcione *et al.* 2018a), which agrees with the results in the plots. For P waves, the phase velocities show a similar behaviour, where μ_c has to be replaced by $K_c + 4\mu_c/3$, and the quality factor is scaled by the quantity $1.5(1 - \bar{\sigma})/(1 - 2\bar{\sigma})$ (see eq. B1).

Next, we consider the solution for the P -wave quality factor of a periodic sequence of slabs of thickness h (fine layering), corresponding to a solution reported by Armstrong (1984, eq. 26; see Appendix C). In this case, only the Grüneisen ratio is allowed to vary. First, we assume properties of the same order of magnitude of the previous example, with $\Gamma_1 = 1.1$, $\Gamma_2 = 2$, $K = \mu = 39 \text{ GPa}$, $c = 106 \times 10^6 \text{ kg m}^{-1} \text{ s}^{-2} \text{ K}^{-1}$, $\gamma/c = 5 \times 10^{-6} \text{ m}^2 \text{ s}^{-1} = 5 \text{ mm}^2 \text{ s}^{-1}$, $E = 91 \text{ GPa}$ and $\rho = 2650 \text{ kg m}^{-3}$. Then, $\gamma = 532 \text{ m kg s}^{-3} \text{ K}^{-1}$, $\beta_1 = c\Gamma_1$, $l = 1, 2$, $\alpha_1 = \beta_1/(3K) = 0.0010 \text{ K}^{-1}$ and $\alpha_2 = \beta_2/(3K) = 0.0018 \text{ K}^{-1}$. Fig. 6 shows the P -wave quality factor as a function of frequency for $h = 0.8$ mm, which is equal to the diameter of the pores considered in one of the previous examples. The Zener fit is also shown, where, in this case, it provides a better match. The higher attenuation at high frequencies implies more dispersion. The attenuation is due to the difference between the Grüneisen ratios of the layers. If this difference is zero, there is no loss, since $Q_0 \rightarrow \infty$ (see eq. C3). The location of the peak is approximately given by eq.

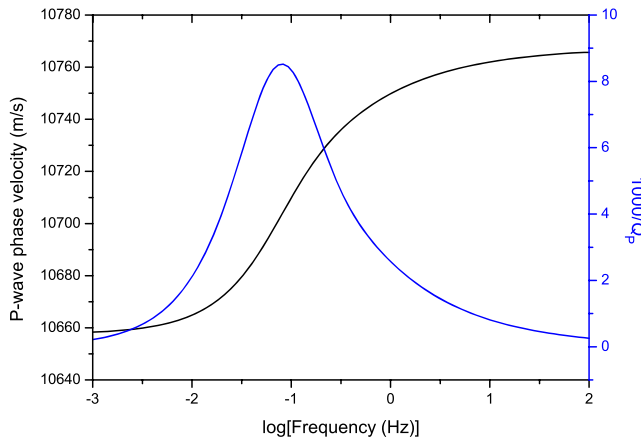


Figure 7. Phase velocity (black curve) and dissipation factor (blue curve) of the P waves as a function of frequency for a periodic sequence of slabs (fine layering). The thickness is $h = 1$ mm (period = 2 mm). The thermoelastic properties correspond to the Earth's mantle (Anderson 2000).

(B6), where in this case $f_0 = 2\gamma/(ch^2)$, that is, the layer thickness is equivalent to the diameter of the cavities. As before, decreasing the size of the layers moves the peak to the high frequencies without affecting the value of the peak quality factor.

Finally we consider a realistic set of properties, related to the Earth's mantle, taken from table 5 in Anderson (2000) (MgSiO₃ perovskite). The notation is such that $\alpha \leftrightarrow 3\alpha$, $\gamma \leftrightarrow \Gamma$, $K_T \leftrightarrow K$, $T \leftrightarrow T_0$, where the left-hand side corresponds to Anderson's notation. For the first layer, we consider the case $T_0 = 500$ K, with $\alpha = 0.00073$ K⁻¹, $\Gamma_1 = 1.37$, $K = 258$ GPa, $\rho = 4087$ kg m⁻³, $\beta = 3\alpha K = 562 \times 10^6$ kg m⁻¹ s⁻² K⁻¹, $c = 410 \times 10^6$ kg m⁻¹ s⁻² K⁻¹ and assume $\gamma = 20.5$ m kg s⁻³ K⁻¹ (Volker *et al.* 2012) and $\mu = 3K/5$ (a Poisson medium). Then, the diffusivity is $\gamma/c = 5 \times 10^{-8}$ m s⁻², $E = 464$ GPa and $c_0 = 10658$ m s⁻¹. The second layer has $\Gamma_2 = 1.8$ and the layer thickness is $h = 1$ mm (period = 2 mm). Fig. 7 shows the phase velocity and dissipation factor of the P waves as a function of frequency. The peak quality factor is $1000/8.3 \approx 117$ at a frequency of 0.08 Hz, in agreement with experimental values in the mantle (e.g. Birch *et al.* 1942; Romanowicz & Mitchell 2007).

Since in Savage (1966) the cavities do not interact, tests of numerical codes, for example, frequency-domain finite-element codes (Santos & Gauzellino 2017), to obtain the complex modulus should be based on a single cavity. The codes can then be used to evaluate the strength of this interaction by including several cavities. The approximations inherent in Armstrong (1984) theory are long wavelengths compared to the size of the layers and negligible variations of the elastic moduli with T (isothermal moduli are appropriate). Moreover, the layers differ only in the values of their Grüneisen ratio.

The analysis can be extended to the case of elliptical cavities (cracks) and a succession of thin layers with a random, uncorrelated distribution of the Grüneisen ratio. Moreover, an alternative theory considering spherical cavities, similar to that of Savage (1966), is that of Panteliou & Dimarogonas (1997), which can be compared to the results obtained in this work. These authors report experimental data. Furthermore, following Mainardi (1994, eq. 24), the heat equation can be generalized so that the relaxation due to the heat diffusion is governed by a fractional differential equation [see also Mainardi (2010), eq. (3.48)]. The solutions can be expressed in terms of Mittag-Leffler functions and a continuous spectrum of relaxation times. The relaxation peak turns out to be broader than

the Debye peak exhibited by the classical Zener model. An application of the fractional model to pressure-diffusion loss can be found in Picotti & Carcione (2017).

4 CONCLUSIONS

We have obtained analytical solutions of the thermoelastic problem in media with cavities or pores (a dry porous medium) and a set of thin periodic layers. The loss mechanism is that of conversion of mechanical energy in the form of deformations and/or waves to the slow thermal mode, similar to the wave-induced fluid-flow attenuation in poroelasticity. Other 'non-Biot' dissipation mechanisms, such as internal friction and local heat flow (squirt flow in poroelasticity), have to be included 'ad hoc' in the background media in the case of cavities and in the single layers in the case of fine layering. Existing solutions provide the quality factor, whereas here we have also obtained the phase velocity and complex modulus as a function of frequency by using the Kramers–Kronig relations. The resulting relaxation curves resemble peaks obtained with the standard-linear solid (Zener) mechanical model, although there are some differences, mainly in the case of cavities.

In the 2-D case (cylindrical pores), the peak is wider and dissipation is weaker compared to the case of spherical 3-D pores, and the P -wave dissipation is smaller than the S -wave one. An example of periodic layers, with realistic values of the thermoelastic properties, typical of the Earth's mantle, gives a P -wave quality factor in agreement with experimental data. In all the cases, the location of the relaxation peaks move to the low frequencies when the size of the pores or the layer thickness increases. Moreover, attenuation (and velocity dispersion) increases with the medium temperature and thermal expansion coefficient.

The solutions obtained herein for these idealized problems provide analytic formulae for the thermal dissipation over the entire frequency range, which are useful to test numerical algorithms, as for instance finite-element harmonic experiments to obtain the bulk and shear complex moduli due to heat currents. This analysis will be extended to the case of elliptical cavities (cracks) and a succession of thin layers with a random, uncorrelated distribution of the Grüneisen ratio.

REFERENCES

- Anderson, O., 2000. The Grüneisen ratio for the last 30 years, *Geophys. J. Int.*, **143**, 279–294.
- Armstrong, B.H., 1984. Models for thermoelastic in heterogeneous solids attenuation of waves, *Geophysics*, **49**, 1032–1040.
- Biot, M.A., 1956. Thermoelasticity and irreversible thermodynamics, *J. Appl. Phys.*, **27**, 240–253.
- Birch, F., Schairer, J.F. & Spicer, H.C., 1942. *Handbook of Physical Constants*, Geological Society of America, Paper 36.
- Carcione, J.M., 2014. *Wave Fields in Real Media. Theory and Numerical Simulation of Wave Propagation in Anisotropic, Anelastic, Porous and Electromagnetic Media*, 3rd edn, extended and revised, Elsevier.
- Carcione, J.M., Santos, J.E. & Picotti, S., 2011. Anisotropic poroelasticity and wave-induced fluid flow. Harmonic finite-element simulations, *Geophys. J. Int.*, **186**, 1245–1254.
- Carcione, J.M., Cavallini, F., Ba, J., Cheng, W. & Qadrouh, A., 2018a. On the Kramers–Kronig relations, *Rheol. Acta*, doi:10.1007/s00397-018-1119-3.
- Carcione, J.M., Wang, Z.-W., Ling, W., Salusti, E., Ba, J. & Fu, L.-Y., 2018b. Simulation of wave propagation in linear thermoelastic media, *Geophysics*, 10.1190/geo2018-0448.1.

- Carcione, J.M., Cavallini, F., Wang, E., Ba, J. & Fu, L.-Y., 2019. Physics and simulation of wave propagation in linear thermo-poroelastic media, *J. geophys. Res.*, doi:10.1029/2019JB017851.
- Chandrasekharaiah, D.S. & Cowin, S.C., 1989. Unified complete solutions for the theories of thermoelasticity and poroelasticity, *J. Elast.*, **21**, 121–126.
- Eshelby, J.D., 1957. The determination of the elastic field of an ellipsoidal inclusion, and related problems, *Proc. R. Soc. A*, **241**, 376–396.
- Landau, L.D. & Lifshitz, E.M., 1970. *Theory of Elasticity*, Pergamon Press.
- Lord, H. & Shulman, Y., 1967. A generalized dynamical theory of thermoelasticity, *J. Mech. Phys. Solid*, **15**(5), 299–309.
- Love, A.E.H., 1944. *Mathematical Theory of Elasticity*, 4th edn, Dover Publications.
- Volker, H., Salanne, M. & Jahn, S., 2012. Thermal conductivity of MgO, MgSiO₃ perovskite and post-perovskite in the Earth's deep mantle, *Earth planet. Sci. Lett.*, **355**, 102–108.
- Mainardi, F., 1994. Fractional relaxation in anelastic solids, *J. Alloys Compd.*, **212**, 534–538.
- Mainardi, F., 2010. *Fractional Calculus and Waves in Linear Viscoelasticity*, Imperial College Press.
- Müller, T.M., Gurevich, G. & Lebedev, M., 2010. Seismic wave attenuation and dispersion resulting from wave-induced flow in porous rocks—a review, *Geophysics*, **75**(5), 75A147–75A164.
- Norris, A.N., 1992. On the correspondence between poroelasticity and thermoelasticity, *J. Appl. Phys.*, **71**, 1138–1141.
- O'Donnell, M., Jaynes, E.T. & Miller, J.G., 1981. Kramers–Kronig relationship between ultrasonic-attenuation and phase-velocity, *J. acoust. Soc. Am.*, **69**, 696–701.
- Panteliou, S.D. & Dimarogonas, A.D., 1997. Thermodynamic damping in porous materials with spherical cavities, *Shock Vib.*, **4**, 261–268.
- Picotti, S. & Carcione, J.M., 2017. Numerical simulation of wave-induced fluid flow seismic attenuation based on the Cole-Cole model, *J. acoust. Soc. Am.*, doi:10.1121/1.4990965.
- Robertson, E.C., 1988. Thermal properties of rocks, USGS open file report 88–441, US Geol Survey, Reston, Virginia.
- Romanowicz, B. & Mitchell, B., 2007. Deep Earth structure: Q of the Earth from crust to core, in *Treatise on Geophysics*, Vol. 1, pp. 731–774, ed. Schubert, G., Elsevier.
- Santos, J.E. & Gazdellino, P.M., 2017. *Numerical Simulation in Applied Geophysics*, Lecture Notes in Geosystems Mathematics and Computing, Birkhauser.
- Savage, J., 1966. Thermoelastic attenuation of elastic waves by cracks, *J. geophys. Res.*, **71**, 3929–3938, Correction: 1967, JGR, **72**, 6387.
- Treitel, S., 1959. On the attenuation of small-amplitude plane stress waves in a thermoelastic solid, *J. geophys. Res.*, **64**, 661–665.
- Zener, C., 1937. Internal friction in solids. I. Theory of internal friction, *Phys. Rev.*, **52**, 230–235.
- Zener, C., 1938. Internal friction in solids. II. General theory of thermoelastic internal friction, *Phys. Rev.*, **53**, 90–99.
- Zener, C., 1946. *Anelasticity of Metals*, American Institute of Mining and Metallurgical Engineers, Pub. no. 1992.
- Zimmerman, R.W., 2000. Coupling in poroelasticity and thermoelasticity, *Int. J. Rock Mech. Min. Sci.*, **37**, 79–87.

APPENDIX A: ANALOGY BETWEEN THE STATIC (DIFFUSIVE) THERMOELASTICITY AND POROELASTICITY FIELDS

Chandrasekharaiah & Cowin (1989) unified in one set of equations the theories of thermoelasticity and poroelasticity, including the properties responsible for attenuation and velocity dispersion, but they do not provide explicit solutions. On the other hand, Norris (1992) established the exact mathematical analogy between the equations of static poroelasticity, but excluded the loss properties.

Here, we obtain an analogy between the respective diffusion equations focused on attenuation and dispersion. Let us consider the thermoelastic case. From eqs (1) and (3), we obtain

$$\partial_i \partial_j \sigma_{ij} = 2\mu \partial_i \partial_j \epsilon_{ij} + \lambda \partial_i \partial_i \epsilon - \beta \Delta T = 0. \quad (\text{A1})$$

Since $\partial_i \partial_j \epsilon_{ij} = \partial_i \partial_i \epsilon = \Delta \epsilon$, we have

$$E \Delta \epsilon - \beta \Delta T = 0, \quad (\text{A2})$$

where $E = \lambda + 2\mu = K + 4\mu/3$. Combining eqs (4) and (A2) and after some calculations, we obtain

$$\dot{\mathcal{T}} = \left(\frac{\gamma}{c + \beta^2 T_0/E} \right) \mathcal{T} = d_t \Delta \mathcal{T} = \partial_i \mathcal{T}, \quad \text{with } \mathcal{T} = \Delta T. \quad (\text{A3})$$

The quantity

$$d_t = \frac{\gamma}{c + \beta^2 T_0/E} \quad (\text{A4})$$

is the corresponding thermal diffusivity. This quantity has been obtained by Zimmerman (2000) in a diffusion equation coupled to the rate of confining pressure (static thermo-poroelasticity) [his eq. (59)], and by Treitel (1959) in his eq. (17) relating the adiabatic P -wave modulus, E_A , to the corresponding isothermal modulus, E , that is, $E_A = E d_t/c$. For zero thermal expansion ($\alpha = 0$, $\beta = 0$), $E_A = E$. Eq. (17) in Carcione *et al.* (2018), relating the adiabatic and isothermal P -wave velocities, is equivalent to Treitel's equation.

In poroelasticity, defining $\mathcal{P} = \Delta p_f$, where p_f is the fluid pressure, we obtain the diffusion equation

$$d_h \Delta \mathcal{P} = \partial_t \mathcal{P}, \quad (\text{A5})$$

where

$$d_h = M \left(\frac{\kappa}{\eta} \right) \left(\frac{K_m + 4\mu_m/3}{K_G + 4\mu_m/3} \right) \quad (\text{A6})$$

is the corresponding hydraulic diffusivity constant, where M is the fluid modulus, η is the fluid viscosity, κ is the hydraulic permeability, K_m and μ_m are the dry-rock bulk and shear moduli, and K_G is the Gassmann bulk modulus. This is given by

$$K_G = K_m + \left(1 - \frac{K_m}{K_s} \right)^2 M, \quad (\text{A7})$$

where

$$M = \frac{K_s}{1 - \phi - K_m/K_s + \phi K_s/K_f}, \quad (\text{A8})$$

ϕ is the porosity, and K_s and K_f are the solid and fluid bulk moduli, respectively (Carcione 2014, eq. 7.336).

Comparing eqs (A3) and (A5), the analogy between T and p_f and d_t and d_h is clear. These diffusivities govern the wave-induced attenuation in thermoelastic and poroelastic media, respectively.

Alternatively, Biot (1956) obtains the analogy between the entropy, s , in thermoelasticity and the variation of fluid content, ζ , in poroelasticity, where

$$\begin{aligned} \frac{cT}{T_0} + \beta \epsilon = s &\leftrightarrow \zeta = \frac{p_f}{M} + \alpha \epsilon, \\ T &\leftrightarrow p_f, \\ 1/M &\leftrightarrow c/T_0, \\ \beta &\leftrightarrow \alpha \end{aligned} \quad (\text{A9})$$

(Biot's eqs 2.14 and 4.6; Carcione 2014, eq. 7.32). Both, s and ζ satisfy diffusion equations similar to eqs (A3) and (A5), respectively.

APPENDIX B: THERMOELASTIC ATTENUATION BY A MEDIUM WITH SPHERICAL AND CYLINDRICAL PORES

Savage (1966) obtained the quality factor of the P and S waves for media filled with spheres (3-D) and cylindrical cavities (2-D) or pores, both of radius a . Eq. (2) in that paper is uniquely identified with the diffusion equation (4) if D , Γ and ρC in Savage (1966) are identified with γ/c , β/c and c in our paper, respectively (ρ is the mass density). Γ is called the Grüneisen ratio (see Appendix C). In Savage (1966), $\Gamma = \alpha_v K/c$, while here $\Gamma = 3\alpha K/c$. This is due to the difference between the linear and volumetric thermal expansion coefficients, α and $\alpha_v = 3\alpha$, respectively.

Savage (1966) considered the (x, y) -plane for both the spherical and circular-cylinder cavities, and an applied plane strain ϵ_{12} . This shear strain produces a dilatation in the cavities, which in turn generates a heat current and a temperature field T . Instead, for an applied pure dilatation (related to the bulk modulus), there is no energy dissipation, that is, when a small spherical cavity is placed in a medium with pure dilation, the only strains introduced by the cavity are pure shears (Love 1944). The same situation happens in a circular-cylinder cavity, where the applied pure dilatation is the 2-D hydrostatic strain $\epsilon_{xx} = \epsilon_{yy}$, $\epsilon_{33} = 0$, and $\epsilon_{ij} = 0, i \neq j$.

B1 Spherical pores

For P waves,

$$Q_P = \frac{3}{2} \cdot \frac{1 - \bar{\sigma}}{1 - 2\bar{\sigma}} \cdot Q_S \quad (\text{B1})$$

where Q_S is the S -wave quality factor given below, and $\bar{\sigma}$ is the relaxed effective Poisson ratio for the porous medium (at zero frequency), given by

$$\bar{\sigma} = \frac{3\bar{K} - 2\bar{\mu}}{2(3\bar{K} + \bar{\mu})}, \quad (\text{B2})$$

where

$$\bar{K} = \frac{K}{1 + \frac{3\phi(1-\sigma)}{2-4\sigma}}, \quad \bar{\mu} = \frac{\mu}{1 + \frac{15\phi(1-\sigma)}{7-5\sigma}} \quad (\text{B3})$$

(Eshelby 1957), ϕ is the porosity, and K and μ are the bulk and shear moduli of the mineral. Eq. (B1) is due to the absence of attenuation related to dilatational deformations, that is, the bulk modulus, \bar{K} , is a real quantity in the frequency domain. If $\nu = c_P/c_S = 2(1 - \bar{\sigma})/(1 - 2\bar{\sigma})$ is the relaxed P/S velocity ratio, and $\text{Re}(\bar{K}) \simeq \rho(c_P^2 - 4c_S^2/3)$ and $\text{Im}(\bar{\mu}) \simeq \rho c_S^2$ (low-loss medium), it can be shown that $\nu(Q_P^{-1} - Q_K^{-1}) = (4/3)(Q_S^{-1} - Q_K^{-1})$. If $Q_K^{-1} = 0$, we obtain eq. (B1).

For S waves,

$$Q_S^{-1} = \frac{16\mu\phi\beta^2 T_0}{3c\bar{\mu}K} \cdot p(\sigma)(1 - 2\sigma)(1 + \sigma)F(\omega), \quad (\text{B4})$$

where

$$p(\sigma) = \frac{135}{4(7 - 5\sigma)},$$

$$F(\omega) = \frac{\chi^2(2\chi^2 + 5\chi + 4)}{[(2\chi^3 - 9\chi - 9)^2 + \chi^2(2\chi^2 + 8\chi + 9)^2]},$$

$$\chi^2 = \frac{\omega c a^2}{2\gamma} \quad (\text{B5})$$

and ω is the angular frequency. The quantities χ , p and F are dimensionless. Pure dilatations do not cause attenuation.

Thermoelastic attenuation peaks approximately at the frequency

$$f_0 = \frac{\gamma}{2ca^2}, \quad (\text{B6})$$

where γ/c is a thermal diffusivity in eq. (4), and $\chi^2 = (\pi/2)(ff_0)$.

B2 Cylindrical pores

For P waves, Q_P is given by eq. (B1). For S waves,

$$Q_S^{-1} = \frac{16\mu\phi\beta^2 T_0}{3c\bar{\mu}K} \cdot (1 - 2\sigma)(1 + \sigma)F(\omega), \quad (\text{B7})$$

where here

$$\bar{\mu} = \frac{\mu}{1 - 4\phi(1 - \sigma)},$$

$$F(\omega) = |b|^{-2} \text{Re} \left[\frac{H_1^{(1)}(b)}{H_2^{(1)'}(b)} \right],$$

$$b = \sqrt{\frac{i\omega c a^2}{\gamma}} = a(1 + i) \sqrt{\frac{\omega c}{2\gamma}}. \quad (\text{B8})$$

where $H_n^{(1)}$ are cylindrical Hankel functions and the prime indicates a derivative with respect to the argument.

The value of the minimum quality factor depends mainly on $\beta = 3\alpha K$, the higher α , the lower the Q factor, see eqs (B4) and (B7). Note also that increasing the absolute temperature T_0 implies higher attenuation.

APPENDIX C: THERMOELASTIC ATTENUATION BY FINE LAYERING

Let us consider a periodic system of alternating layers (slabs) each with thickness h , much smaller than the signal wavelength. We assume that the attenuation is small, that is, $Q \gg 1$. Armstrong obtained the relaxation peak caused by the passage of a P wave. There is an induced temperature variation, which in turn induces a heat current and attenuation. Due to the different notations, we compare our eq. (4) to eq. (1) in Armstrong (1984). The equivalence is $\chi \leftrightarrow \gamma/c$, $\gamma \leftrightarrow \beta/c$ and $\kappa \leftrightarrow \gamma$, where the left-hand side properties correspond to those of Armstrong (1984). He gives the result for the case where only the Grüneisen ratio,

$$\Gamma = \frac{\beta}{c} \quad (\text{C1})$$

(dimensionless) varies from slab to slab.

For cyclic boundary conditions of continuity of temperature and thermal current, we have

$$Q_P = \frac{q(\cosh q + \cos q)}{\sinh q - \sin q} \cdot Q_{P0}, \quad q = h \sqrt{\frac{\omega c}{2\gamma}}, \quad (\text{C2})$$

where

$$Q_{P0} = \frac{4E}{cT_0(\Gamma_2 - \Gamma_1)^2}, \quad (\text{C3})$$

$$E = K + \frac{4}{3}\mu \quad (\text{C4})$$

is the relaxed P -wave modulus.

APPENDIX D: ZENER MECHANICAL MODEL

The Zener or standard-linear-solid model can be used to approximate the quality factors. The complex modulus of the Zener model

is

$$M(f) = \frac{Q_0 + i(f/f_0)(R + 1)}{Q_0 + i(f/f_0)(R - 1)} \cdot M_0, \quad R = \sqrt{1 + Q_0^2}, \quad (\text{D1})$$

where f_0 is the relaxation frequency, Q_0 is the minimum quality factor at f_0 , M_0 is the zero-frequency modulus, f is the frequency and $i = \sqrt{-1}$. The unrelaxed modulus ($f \rightarrow \infty$) is $M_\infty = [(R + 1)/(R - 1)]M_0$, and the following relations holds, $Q_0 = 2\sqrt{M_\infty M_0}/(M_\infty - M_0)$, so that the modulus dispersion $M_\infty - M_0$ can approximately be obtained from Q_0 . Eq. (D1) has been obtained by Zener (1937) for a rod of arbitrary cross-section vibrating transversely, where M_0 and M_∞ correspond to the isothermal and adiabatic moduli [Zener (1938); Mainardi (2010), eq. (3.41)].

The Zener Q factor is

$$Q_Z = \frac{\text{Re}(M)}{\text{Im}(M)} = \frac{Q_0}{2} \cdot \frac{1 + (f/f_0)^2}{f/f_0} \quad (\text{D2})$$

(e.g. Carcione 2014), and the phase velocity is

$$c_{\text{ph}} = \left[\text{Re} \left\{ \frac{1}{v_c} \right\} \right]^{-1}, \quad v_c = \sqrt{\frac{M}{\rho}}, \quad (\text{D3})$$

where v_c is the complex velocity and ρ is the mass density (e.g. Carcione 2014).